

### Supplementary figure captions

Fig.1 X-ray diffraction pattern performed on  $\text{Ni}_3\text{TeO}_6$  crystal powder (lower) and  $\text{Ni}_3\text{TeO}_6$  single crystal having (003) orientation (upper).

Fig. 2 Peak Indices of x-ray diffraction pattern of  $\text{Ni}_3\text{TeO}_6$  crystal powder.

Fig. 3 Superimposed x-ray diffraction patterns of (101) & (b) (003) planes  $\text{Ni}_3\text{TeO}_6$  single crystals.

Fig. 4 Thermal variations of derivative of dc magnetic susceptibility carried out on  $\text{Ni}_3\text{TeO}_6$  single crystal in the parallel and perpendicular directions.

Fig.5 Magnetization curves of  $\text{Ni}_3\text{TeO}_6$  single crystal in the parallel and perpendicular directions at 10 K.

Fig. 6 Temperature dependence of the dc magnetic susceptibility  $\chi$  of  $\text{Ni}_3\text{TeO}_6$  (003) plane single crystal, measured employing a weak magnetic field of 100 Oe in the perpendicular direction. Two anomalies at 60 and 52 K are clearly evident in the inset.

Fig. 7 Temperature dependence of the dc magnetic susceptibility  $\chi$  of  $\text{Ni}_3\text{TeO}_6$  (003) plane single crystal, measured employing a strong magnetic field of 10000 Oe in both the parallel and perpendicular direction. Only one anomaly at 52 K is seen.

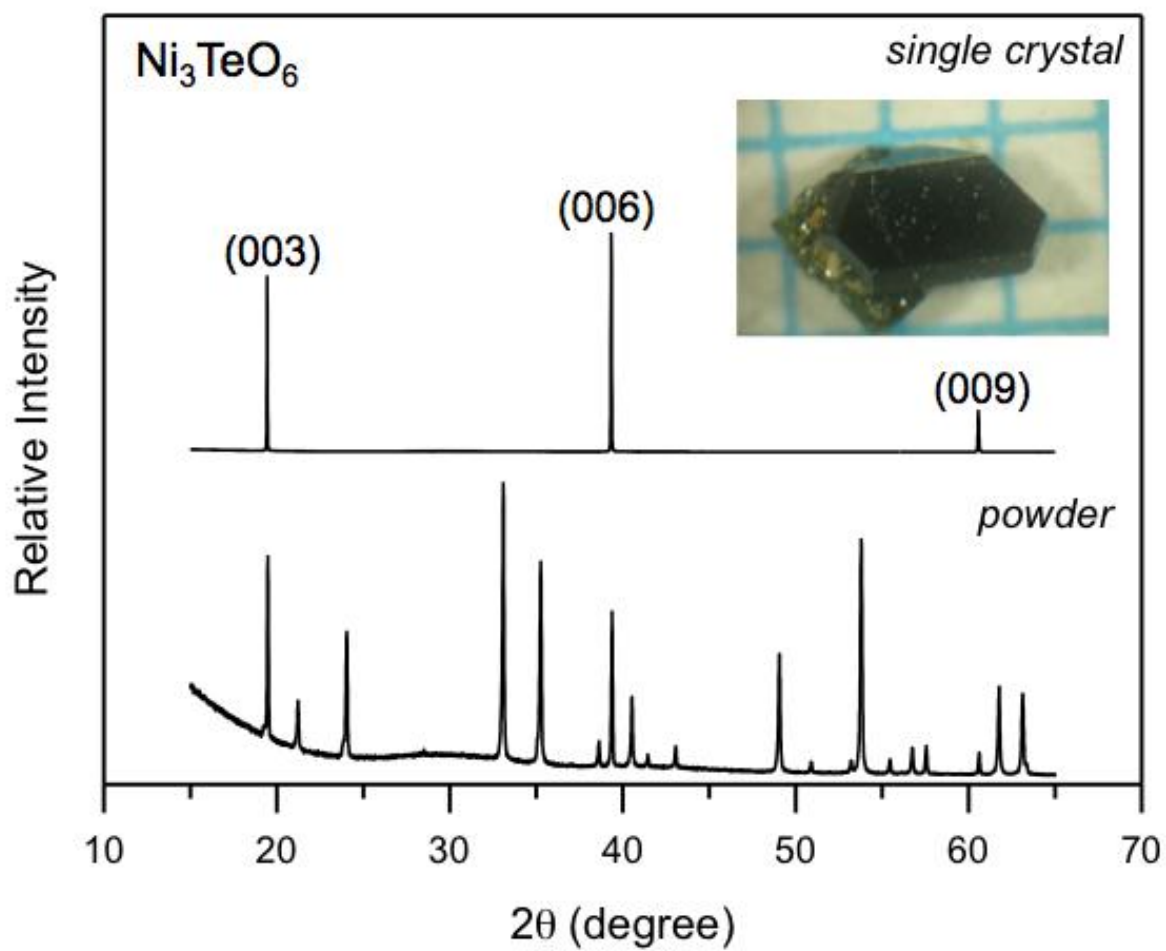


FIG. 1

# Ni<sub>3</sub>TeO<sub>6</sub>

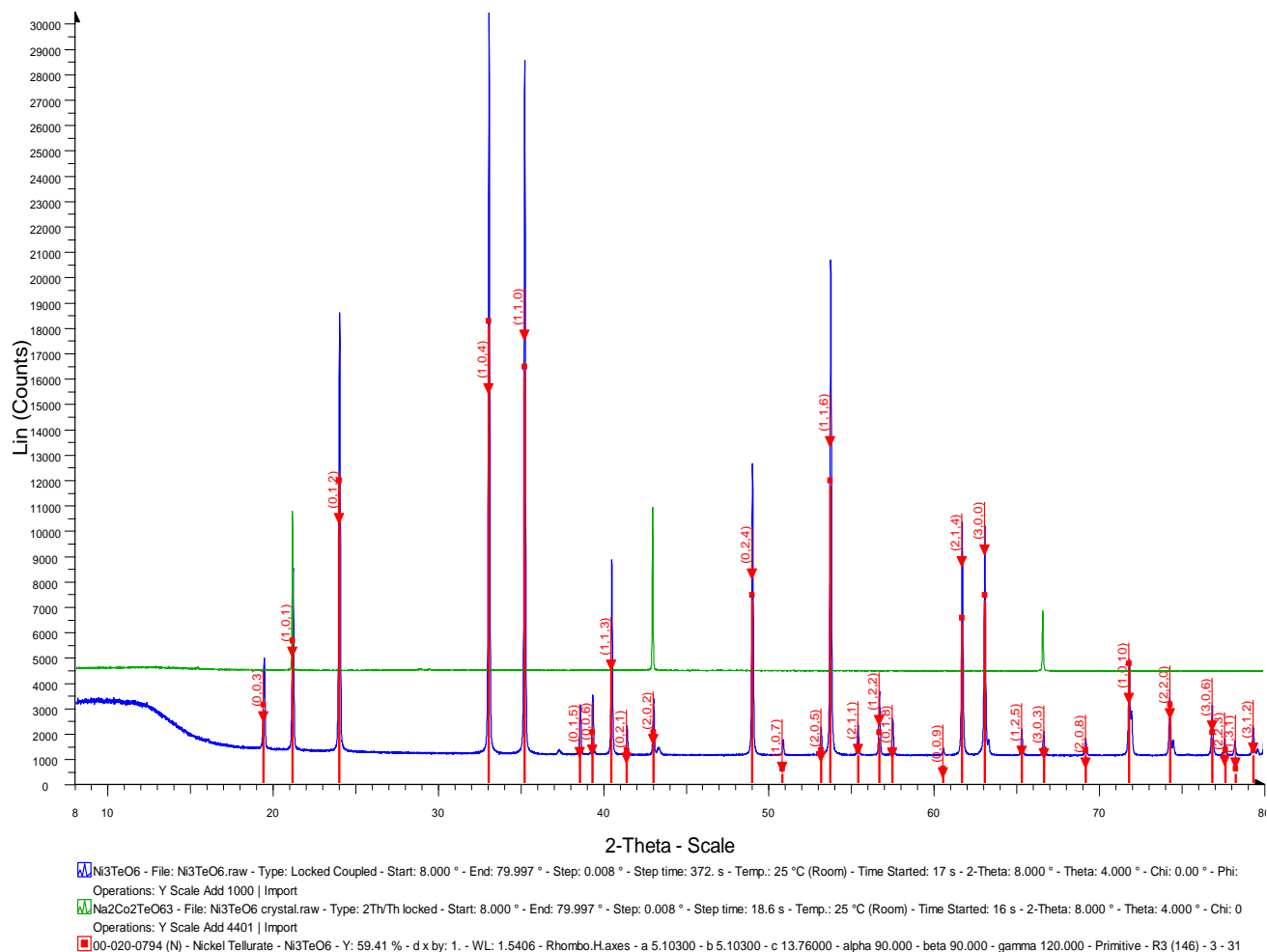


FIG: 2

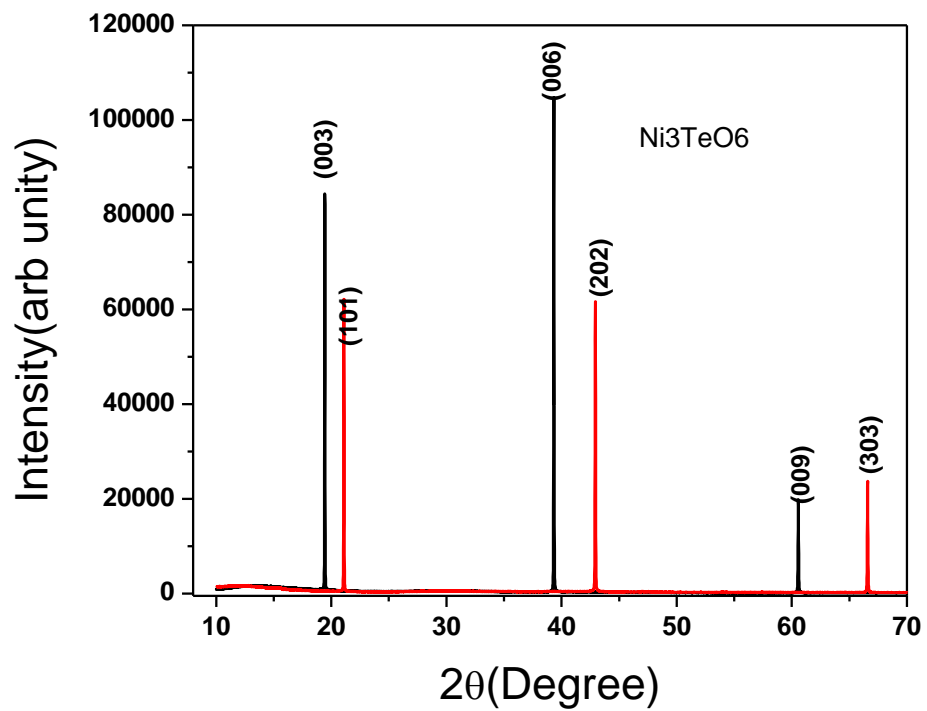


FIG:3

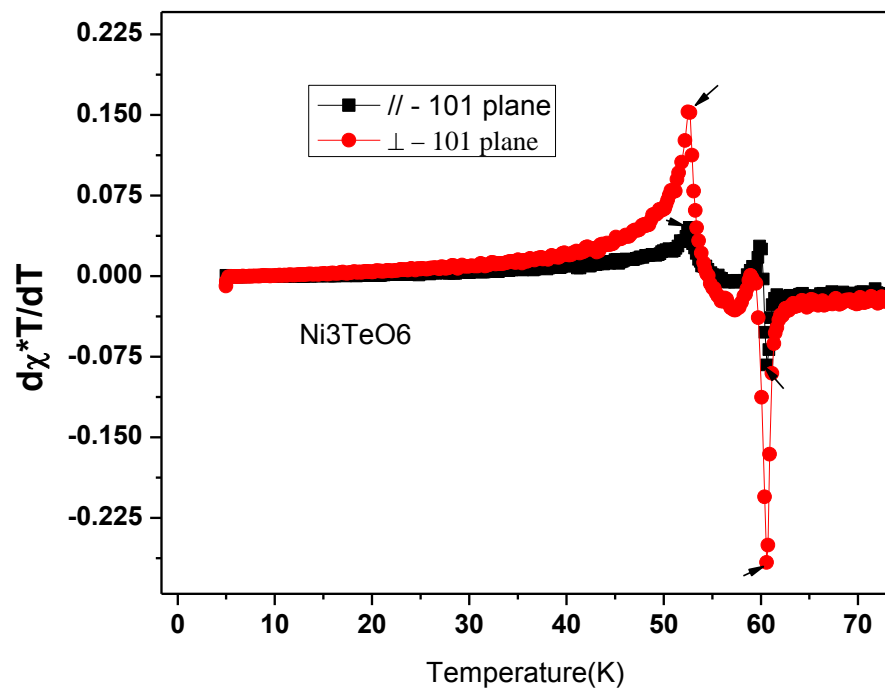


FIG: 4

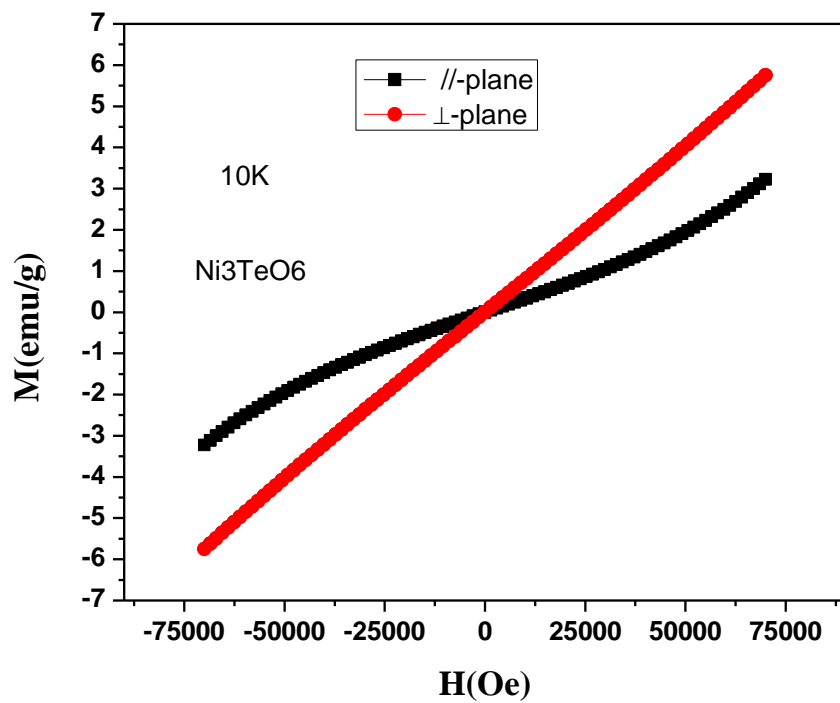


Fig : 5

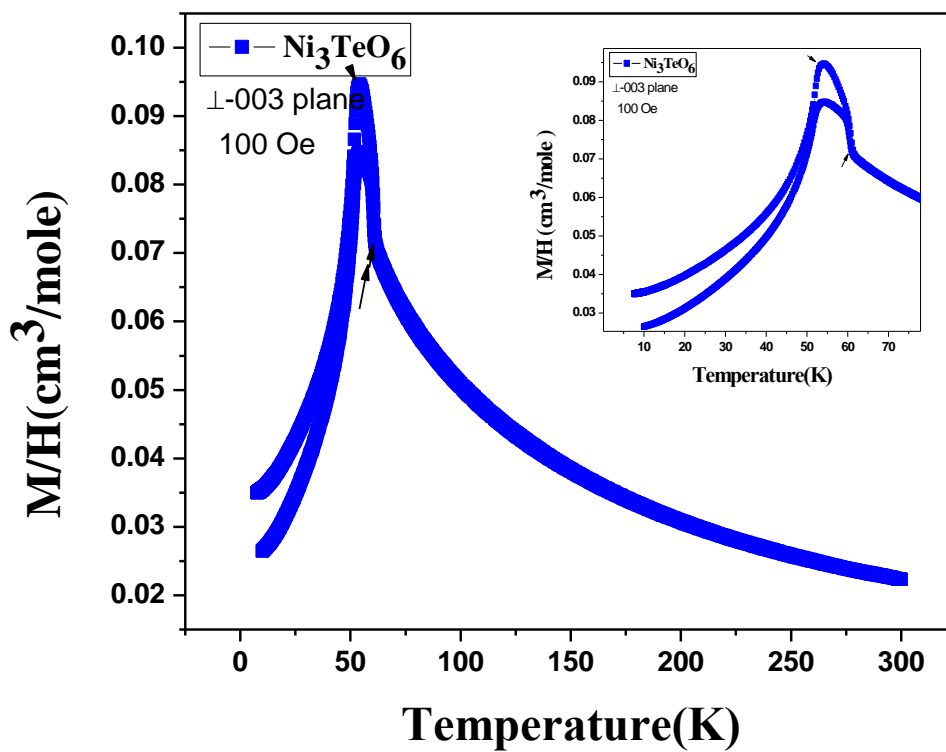


FIG: 6

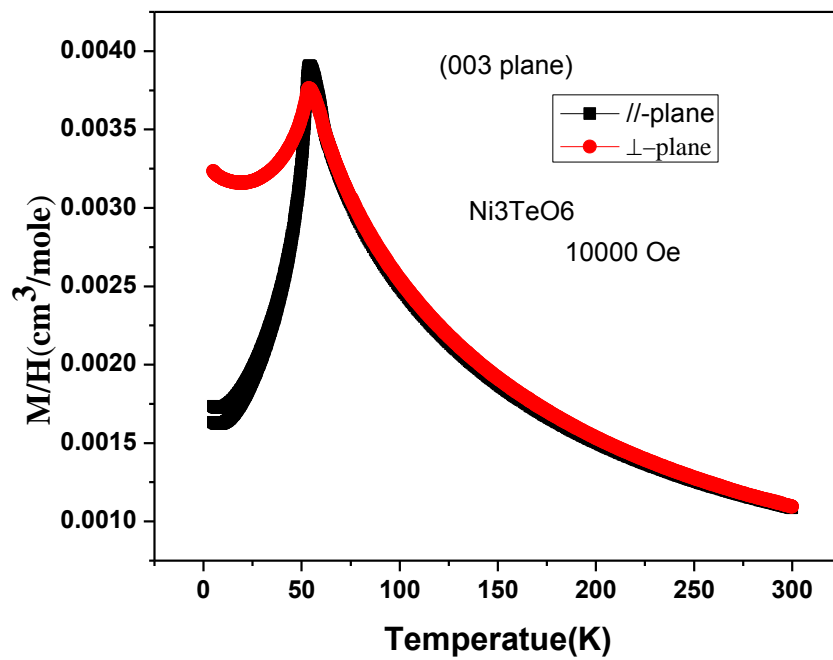


FIG:7